A numerical approach for injection molding of short-fiber-reinforced plastics using a particle method

Yashiro, Shigeki
Faculty of Engineering, Shizuoka University

Okabe, Tomonaga
Department of Aerospace Engineering, Tohoku University

Matsushima, K.
Department of Mechanical Engineering and Sciences, University of Toyama

出版情報：Advanced Composite Materials. 20 (6), pp.503-517, 2012-04-02. Taylor and Francis
バージョン：
権利関係：

Advanced Composite Materials 20 (2011) 503–517
DOI:10.1163/092430411X584423

A numerical approach for injection molding of short-fiber-reinforced plastics using a particle method

S. Yashiro [a,*], T. Okabe [b] and K. Matsushima [c]

[a] Faculty of Engineering, Shizuoka University, 3-5-1 Johoku, Naka-ku, Hamamatsu 432-8561, Japan

[b] Department of Aerospace Engineering, Tohoku University, 6-6-01 Aoba-yama, Aoba-ku, Sendai, 980-8579, Japan

[c] Department of Mechanical Engineering and Sciences, University of Toyama, Gofuku 3190, Toyama-shi, Toyama 930-8555, Japan

* Corresponding author: Tel: +81-53-478-1026; Fax: +81-53-478-1026.

E-mail address: tsyashi@ipc.shizuoka.ac.jp (S. Yashiro)

Abstract

This study proposes a numerical approach for predicting the injection molding process of short-fiber-reinforced plastics using the moving particle semi-implicit (MPS) method, which is a particle-simulation method. Unlike conventional methods using orientation tensors, this approach represents all fibers and resin as an assembly of particles, and automatically analyzes the interaction between fiber and resin and between fibers. In addition, this method can follow the motion of a specific fiber, which is a significant advantage over orientation tensors. This study simulated the injection molding of short-fiber-reinforced plastics; the thermoplastic resin was considered as an incompressible viscous fluid and the fibers were modeled as rigid bodies. The numerical result illustrated that the molding material was unidirectionally reinforced by short fibers since the fibers rotated and were aligned parallel to

the flow direction due to the velocity gradient near the wall boundary. Moreover, the stagnation of resin at a corner was predicted. The results agreed well with previous studies, and the present approach was confirmed. Beyond this, we predicted the accumulation of fibers near the wall due to the velocity gradient, which could not be represented by conventional simulations based on orientation tensors.

Keywords: Polymer-matrix composites (PMCs), Short-fiber composites, Injection molding, Numerical analysis, Microstructures.

1. Introduction

Injection-molded short-fiber-reinforced plastics have various advantages, such as low molding cost, high molding flexibility, and a fast molding cycle. They have been used in various applications, such as components of automobiles, housings for electrical devices, and internal structural components of precision instruments, because of their stiffness and strength. Increasing usage of these composites is now expected, taking advantage of their benefits.

The mechanical properties of injection-molded short-fiber-reinforced plastics are significantly dependent on the reinforcing structure in the material, i.e., the length, distribution, and orientation of the reinforcing fibers. The microscopic structure is generally governed by the molding process. If relatively long fibers (e.g., a few millimeters) are used for a thinner mold, fibers accumulate and fracture during resin flow, and the obtained mechanical properties are often less than the intended values. Accordingly, many studies have been conducted to clarify the process of injection molding of short-fiber-reinforced plastics.

The orientations of reinforcing fibers and their rheological properties have frequently been studied. Advani and Tucker [1] introduced orientation tensors to efficiently represent fiber

orientations. They formulated the equation of change for the orientation tensors by combining the equation of fiber motion with the continuity equation for the total amount of fibers. In addition, methods to approximate the fourth-order tensor from the second-order tensor were introduced to calculate the rate of change in the second-order tensor, and the prediction accuracy of elastic constants was discussed using the approximated fourth-order tensor. Since the orientation tensors provide a convenient way to represent the fiber orientation, they have been widely used for predicting the microscopic structure [2-8]. Gupta et al. [2] calculated the fiber orientation using the second-order tensor and considering the interaction between fibers, and compared the calculation with an experiment with injection-molded plates. In sum, numerical approaches to predicting fiber orientations have been developed based on the orientation tensors and fluid dynamics. However, these approaches ignore fiber motion in the flow analysis, i.e., the flow field is first calculated without fibers and the fiber orientation is then estimated from the obtained flow field. This approach could not represent the actual phenomenon with high fiber content. Chung and Kwon [3] formulated a prediction of fiber orientation that was combined with a flow analysis in order to take the interaction between the fiber and the flow into account, and demonstrated the simulation of injection molding using a thin plate mold. Furthermore, the estimation of rheological properties considering the viscoelastic behavior of resin [4], the improvement of interaction between fibers for a large fraction of fibers [5], and improvement in the approximation of the fourth-order tensor [6,7] have been discussed. Although the methods based on the orientation tensors could easily calculate the fiber orientation, they could not represent a more detailed microscopic structure like the distributed state of the fibers. The orientation tensor did not model the individual fibers, and thus the motion of a specific fiber could not be obtained.

Understanding the mechanisms of fiber motion in resin flow is important for discussing

phenomena concerning fibers such as accumulation. Nonuniform distribution of fiber content is generated when a flow path is chocked with fibers. In addition, fiber accumulation induces deformation and fracture of fibers that significantly affect the quality of molded materials. Yamamoto et al. [8-10] proposed a particle simulation method for analyzing the fiber motion: they modeled the fibers as an assembly of particles and solved the equations of motion for each particle. They predicted the microscopic structure and rheological properties of a molded material. Their approach could represent the accumulation, deformation, and fracture of fibers because the individual fibers were modeled. Furthermore, analysis of high fiber content was made possible by considering the interactions within a fiber and between fibers. However, this approach analyzed the flow and the fiber motion separately, and the change in the flow field due to the fiber orientation could not be represented.

If the motion of the fibers and resin is accurately predicted during the molding process, it becomes possible to improve the material properties, in addition to predicting them, through control of the molding process. This study proposes a numerical simulation for injection molding of short-fiber-reinforced plastics using the moving particle semi-implicit (MPS) method [12-14], which represents a continuum as an assembly of the particles and analyzes the motion of the particles. This particle-simulation method represents all fibers and resin by particles, and the interaction between fibers is thus automatically considered. Moreover, this method can follow the motion of a specific fiber and reproduce the accumulation of fibers, both of which were impossible for simulations based on orientation tensors. Although this study assumes fibers to be rigid bodies for simplicity, fiber fractures during resin flow will be reproduced by representing fibers as elastic bodies. This study first introduces the numerical approach for predicting the molding process of short-fiber-reinforced plastics using the MPS method. Some simulated results are then demonstrated for injection molding with plate and

other molds, and our proposed approach is verified.

2. Moving particle semi-implicit (MPS) method

2.1 Models for differential operators

In particle-simulation methods, a continuum is represented by an assembly of particles and the governing differential equations are discretized by these particles. This section describes the models for differential operators represented by the interaction between neighboring particles [14]. The discretization approach using particles basically differs from mesh-based methods such as the finite-element method and the finite-difference method.

A particle nearer to particle i is assumed to have a greater influence on particle i, and a weight function $w(r)$ is defined as

$$w(r)=\begin{cases} r_e/r-1 & (0<r\le r_e) \\ 0 & (r_e<r) \end{cases}, \tag{1}$$

where r is the distance from particle i. This function represents the magnitude of the influence on particle i. As indicated by Eq. (1), the influences of particles within the radius r_e are considered (Fig. 1). The particle number density n is defined by the sum of the weight function:

$$n_i=\sum_{j\neq i} w\left(\left|\mathbf{r}_j-\mathbf{r}_i\right|\right), \tag{2}$$

where $\mathbf{r}$ denotes the position vector, and the subscript is the particle number. The particle number density is proportional to the density of the fluid.

This study assumes the resin flow to be an incompressible flow. The calculation for incompressible flow uses the gradient and the Laplacian operators, as described later. When particle i and a neighboring particle j have scalar variables ϕ_i and ϕ_j, the gradient model $\langle\nabla\phi\rangle$ at particle i is given by

$$\langle \nabla \phi \rangle_i = \frac{d}{n_0} \sum_{j \neq i} \left[\frac{\phi_j - \phi_i}{\left| \mathbf{r}_j - \mathbf{r}_i \right|^2} \left(\mathbf{r}_j - \mathbf{r}_i \right) w\left(\left| \mathbf{r}_j - \mathbf{r}_i \right| \right) \right]. \tag{3}$$

Here, d is the dimension number, and n_0 is the averaged particle number density. The gradient model represents the weighted mean of the gradient vector between two particles i and j considering the dimensional information (Fig. 2a). The Laplacian model $\langle \nabla^2 \phi \rangle$ is written as

$$\langle \nabla^2 \phi \rangle_i = \frac{2d}{\lambda n_0} \sum_{j \neq i} \left[\left(\phi_j - \phi_i \right) w\left(\left| \mathbf{r}_j - \mathbf{r}_i \right| \right) \right]. \tag{4}$$

This model assumes that part of the variable ϕ of particle i is divided among the neighboring particles considering the weight function (Fig. 2b). A coefficient λ is introduced to cause the increase in statistical dispersion to conform to the analytical solution.

$$\lambda = \sum_{j \neq i} \left| \mathbf{r}_j - \mathbf{r}_i \right|^2 w\left(\left| \mathbf{r}_j - \mathbf{r}_i \right| \right) \Big/ \sum_{j \neq i} w\left(\left| \mathbf{r}_j - \mathbf{r}_i \right| \right) \tag{5}$$

Physical quantities such as velocities are obtained by applying the differential-operator models, Eqs. (3) and (4), to the governing equations.

2.2 Governing equations for incompressible flow

The governing equations for incompressible flow are the conservation of mass and the Navier-Stokes equation.

$$\frac{D\rho}{Dt} = 0 \tag{6}$$

$$\frac{D\mathbf{u}}{Dt} = -\frac{1}{\rho} \nabla P + \nu \nabla^2 \mathbf{u} + \mathbf{g} \tag{7}$$

Here, ρ is density, $\mathbf{u}$ is the velocity, P is the pressure, v is the dynamic coefficient of viscosity, and $\mathbf{g}$ is the acceleration of gravity. D/Dt denotes a Lagrangian differential in the particle-simulation method. The first term of Eq. (7) is the pressure term, the second is the viscosity term, and the third is the gravity term. The equation for conservation of mass for

compressible flow is used instead of Eq. (6) to employ the semi-implicit simulation algorithm described later.

$$\frac{D\rho}{Dt} + \rho \nabla \cdot \mathbf{u} = 0 \tag{8}$$

This study analyzed the reinforcing fibers by assuming rigid bodies. The interaction between the fluid and the rigid bodies is considered to be small, and the motion of particles consisting of rigid bodies is analyzed by Eqs. (7) and (8) for fluid. Next, the relative positions of particles for a rigid body are corrected to restore its original shape, preserving the changes in the coordinates of the gravity point and the rotation angle. This operation corresponds to analyzing the motion of the gravity point of a rigid body by integrating the forces acting on the rigid body from the fluid and other rigid bodies. The above method provides explicit interaction (weak coupling) between the incompressible fluid and the rigid bodies [14].

2.3 Numerical algorithm

This section describes the analysis procedure for solving the governing equations. When the position $\mathbf{r}_i^k$, velocity $\mathbf{u}_i^k$, and pressure P_i^k of particle i are known, where k denotes the time step, Eq. (7) can be divided into two parts: explicitly calculated terms and an implicitly calculated term. First, the viscosity term and the gravity term are explicitly integrated, and a temporary velocity $\mathbf{u}^*$ and position $\mathbf{r}^*$ are obtained.

$$\mathbf{u}^* = \mathbf{u}^k + \Delta t \left[\nu \nabla^2 \mathbf{u} + \mathbf{g} \right]^k \tag{9}$$

$$\mathbf{r}^* = \mathbf{r}^k + \Delta t \, \mathbf{u}^* \tag{10}$$

Here, Δt is the time increment. The Laplacian model, Eq. (4), is applied to calculate the viscosity term. Although the particle number density must be constant because of the condition of constant density, the temporary particle number density n^* differs from the

constant value n_0 after the explicit calculation. Next, the particle number density is corrected to n_0 by modifying the pressure distribution in the following implicit calculation. The particle number density and the velocity at time step (k+1) are written as

$$n_0 = n^{k+1} = n^* + n', \qquad \mathbf{u}^{k+1} = \mathbf{u}^* + \mathbf{u}', \tag{11}$$

where n' and $\mathbf{u}'$ are the amount of correction for the particle number density and velocity. Here, the correction of the velocity is assumed to be generated by the pressure term of Eq. (7).

$$\mathbf{u}' = -\frac{\Delta t}{\rho_0}\nabla P^{k+1} \tag{12}$$

The following equation is then obtained by considering the mass conservation for compressible flow, Eq. (8), and the fact that the density is proportional to the particle number density.

$$\frac{n'}{n_0 \Delta t} + \nabla \cdot \mathbf{u}' = 0 \tag{13}$$

Equation (12) is substituted into Eq. (13), resulting in a system of linear equations about the unknown pressure P_i^{k+1} using the Laplacian model.

$$\left\langle \nabla^2 P \right\rangle_i^{k+1} = \frac{2d}{\lambda n_0} \sum_{j \neq i} \left[\left(P_j^{k+1} - P_i^{k+1} \right) w\left(\left| \mathbf{r}_j^* - \mathbf{r}_i^* \right| \right) \right] = -\frac{\rho_0}{(\Delta t)^2} \frac{n_i^* - n_0}{n_0} \tag{14}$$

The pressure is implicitly solved, and the acceleration $D\mathbf{u}/Dt$ at time step k is obtained by substituting the calculated pressure into Eq. (7). The velocity $\mathbf{u}$ and the position $\mathbf{r}$ are finally updated using the Newmark method.

The translational and rotational motions of rigid fibers are interacted explicitly with resin flow. The particles within rigid bodies are first analyzed by the above algorithm for incompressible flow in each time step. After finishing the flow analysis at each time step, the relative positions among the particles of a rigid body are corrected to restore the original shape. Here, changes in the coordinates of the gravity point and the rotation angle are

preserved.

A flowchart of the analysis is presented in Fig. 3. After inputting the initial conditions, the gravity term and the viscosity term are first explicitly calculated for all particles, and then the particles are temporarily moved. Here, the mass-conservation condition cannot be satisfied by the temporary geometry. The Poisson equation for pressure is then implicitly solved to satisfy the mass conservation; this study used the ICCG method to solve Eq. (14). Once the pressure is obtained, the acceleration is then calculated by Eq. (7), and the velocity and coordinate of each particle are updated using the Newmark method. Thus, the resin flow is analyzed by this semi-implicit simulation algorithm. Finally, the relative positions among the particles of a rigid body are modified to restore the original shape of the rigid body.

3. Numerical analysis

3.1 Analytical model

A two-dimensional analysis for injection molding of short-fiber-reinforced plastics was conducted. The analysis model is depicted in Fig. 4a. Polypropylene (PP) was assumed to be an incompressible viscous fluid (i.e., a Newtonian fluid), and glass fibers (GF) were modeled by rigid bodies. These materials, allocated in a resin bath 30 mm wide, were pushed by a moving rigid wall to pass a gate 6 mm wide and to fill a plate mold 80 mm long and 4 mm wide. The particle size was 0.25 mm; there were 18,066 particles in this model. The density of the resin was 900 kg/m^3, and its coefficient of viscosity was 900 Pa·s [15]; the density of the glass fiber was 2540 kg/m^3. The weight fraction of fibers was 10%, which corresponded to a 3.8% volume fraction. The length of all fibers was assumed to be 1 mm. The fibers were positioned randomly and were aligned in the direction vertical to the injection (y-direction) as the initial condition.

Many corners and branches exist in practical injection molding. In order to predict the resin flow at these parts, a corner model (Fig. 4b, 18,066 particles) and a branch model (Fig. 4c, 19,026 particles) were also analyzed.

The rigid wall was moved at an initial speed of 1 m/s to fill the mold. Particles with unrealistic pressure increased with this injection speed, and practical results could not be obtained. The injection speed was then decreased to 60% of the original value when the maximum pressure reached the baseline, and the maximum value was set to the baseline. Thus, the molding process was adjusted by stepwise decreases in the injection speed according to the increase in pressure.

3.2 Analytical results and discussion

Figure 5 depicts the predicted resin flow during injection into a plate mold. The injection speed gradually decreased with increasing pressure until the resin passed the gate (0.015 s). The resin started to fill the mold after 0.02 s and completely filled it at 0.16 s. Fibers were aligned with the flow (x) direction when the resin passed the gate and were rotated in the y-direction when the resin reached the bottom wall of the inlet. The flow direction changed during the interval from 0.025 to 0.03 s. The behavior of the fibers injected afterward was the same as that of the foregoing fibers. Therefore, fibers aligned in the y-direction were observed in the filled materials (0.06 to 0.12 s). This fiber motion was caused by the velocity distribution due to viscosity; the flow velocity was low near the wall and increased with distance from the wall, as indicated in Fig. 5b. The fibers were then rotated to the flow direction and were aligned unidirectionally [2,16]. In the case of three-dimensional simulations, resin flow in the depth (z) direction of the mold could not be generated if the size in the z-direction was similar to that of the gate, and results similar to Fig. 5 would be

obtained. When the depth was great compared to the gate, flow in the *z*-direction would occur, and fibers would be moved by the same mechanism as in Fig. 5. In this case, the fibers will be aligned in the *yz*-plane.

In the predicted resin flow depicted in Fig. 5, fibers accumulated near the side wall as seen in the magnified view (Fig. 6). The flow velocity was low near the wall due to viscosity, and fibers #2 and #3 moved slowly. The fibers farther from the side wall (#1) overtook the fibers #2 and #3 because of their greater velocity. These fibers are positioned within a short distance in Fig. 6, and the backward #1 fiber collided with fibers #2 and #3. Free motion of these fibers was prevented, and the fibers accumulated. This phenomenon could not be represented by any analysis based on the fiber-orientation tensors [1-7].

Figure 7 depicts the resin flow and velocity distribution in a mold with corners at 0.18 s when the mold was almost filled. Similarly to the plate mold depicted in Fig. 5, the fibers were almost aligned with the flow direction, and were oriented parallel to the side wall of the flow path (Fig. 7a). Moreover, the velocity was almost zero at the corner, and stagnation of resin was observed as depicted in Fig. 7b. These predictions agreed with the resin flow observed by Yamamoto et al. [10]. Stagnation of fibers did not appear at the corner since the fiber content was low in this simulation.

The resin flow and velocity distribution in a mold with branches are depicted in Fig. 8. Fibers moved forward and were aligned parallel to the side wall before reaching the branch. However, unlike the resin flow in the plate and corner molds, some fibers (indicated by arrows in Fig. 8a) had a large angle from the flow direction after passing the branch. The velocity vector was inclined from the original flow direction (*y*) to the branched direction (*x*), as indicated in the velocity distribution in Fig. 8b. Thus, this velocity distribution yielded some inclined fibers near the branch, although the fibers gradually aligned with the side wall

after passing the branched flow path.

4. Conclusions

This study proposed a numerical analysis to predict resin flow and fiber motion during injection molding of short-fiber-reinforced plastics using the moving particle semi-implicit (MPS) method, which is a particle simulation method. We investigated the fiber motion in detail and compared predictions with previous studies. The conclusions are summarized below.

1. This analysis represented the fiber motion by actually modeling the fibers. Individual fibers were unidirectionally oriented, since fibers were rotated to the flow direction because of the velocity gradient caused by viscosity.
2. Backward fibers collided with forward-moving fibers near the wall due to the velocity distribution in the width direction of the flow path, and an accumulation of fibers was predicted. This phenomenon could not be represented by conventional approaches based on fiber-orientation tensors.
3. In a mold with corners, fibers almost aligned with the flow direction, and stagnation was observed at the corner.
4. Fibers that had a large inclined angle from the wall were predicted near the branch because of the velocity distribution.

These conclusions agreed with previous studies, and the proposed simulation was confirmed. Furthermore, this method reproduced an accumulation of fibers that could not be illustrated by conventional approaches. In addition, depending on the molding conditions, variations in fiber length can appear in molded materials due to fiber breakages. This phenomenon would influence the flow process and the local microscopic structure, and

eventually the mechanical properties of the molding materials. A particle-simulation method has an absolute advantage over conventional approaches: variations in short fibers can be realistically modeled, and their influence is automatically analyzed. Thus, the present simulation method can be a strong candidate for predicting molding processes.

References

[1] S. G. Advani, C. L. Tucker III, The use of tensors to describe and predict fiber orientation in short fiber composites, *J. Rheology* 31(8), 751-784 (1987).

[2] M. Guputa, K. K. Wang, Fiber orientation and mechanical properties of short-fiber-reinforced injection-molded composites: simulated and experimental results, *Polym. Compos.* 14(5), 367-382 (1993).

[3] S. T. Chung, T. H. Kwon, Coupled analysis of injection molding filling and fiber orientation, including in-plane velocity gradient effect, *Polym. Compos.* 17(6), 859-872 (1996).

[4] A. Ramazani, A. Ait-Kadi, M. Grmela, Rheological modelling of short fiber thermoplastic composites, *J. Non-Newtonian Fluid Mech.* 73(3), 241-260 (1997).

[5] X. Fan, N. Phan-Thien, R. Zheng, A direct simulation of fibre suspensions, *J. Non-Newtonian Fluid Mech.* 74(1-3), 113-135 (1998).

[6] K.-H. Han, Y.-T. Im, Numerical simulation of three-dimensional fiber orientation in short-fiber-reinforced injection-molded parts, *J. Mater. Process. Technol.* 124(3), 366-371 (2002).

[7] D. Dray, P. Gilormini, G. Régnier, Comparison of several closure approximations for evaluating the thermoelastic properties of an injection molded short-fiber composite, *Compos. Sci. Technol.* 67(7-8), 1601-1610 (2007).

[8] S. Yamamoto, T. Matsuoka, Dynamic Simulation of microstructure and rheology of fiber suspensions, *Polym. Eng. Sci.* 36(19), 2396-2403 (1996).

[9] S. Yamamoto, T. Matsuoka, Dynamic simulation of rod-like and plate-like particle dispersed systems, *Comput. Mater. Sci.* 14(1-4), 169-176 (1999).

[10] S. Yamamoto, Y. Inoue, T. Higashi, T. Matsuoka, Microstructure prediction of injection molded parts of particle dispersed thermoplastics by particle simulation method, *Trans. Japan Soc. Mech. Eng. A* 65(651), 506-513 (1999) (in Japanese).

[11] S. Yamamoto, Development and application of the particle simulation method for fiber and platelike particle dispersed systems, *J. Soc. Rheology, Japan* 29(4), 185-190 (2001).

[12] S. Koshizuka, A. Nobe, Y. Oka, Numerical analysis of breaking waves using the moving particle semi-implicit method, *Int. J. Numer. Meth. Fluids* 26(7), 751-769 (1998).

[13] Y. Chikazawa, S. Koshizuka, Y. Oka, A particle method for elastic and visco-plastic structures and fluid-structure interactions, *Comput. Mech.* 27(2), 97-106 (2001).

[14] S. Koshizuka, Particle Simulation Method, Maruzen, Tokyo (2005).

[15] V. Michaud, A. Mortensen, Infiltration processing of fibre reinforced composites: governing phenomena, *Compos. Part A* 32(8), 981-996 (2001).

[16] D. Hull, T. W. Clyne, An Introduction to Composite Materials (2nd Ed.), Cambridge University Press, New York (1996).

Figure captions

Figure 1 Schematic diagram of the interaction between neighboring particles.

Figure 2 Particle-interaction models for differential operators.

Figure 3 Flowchart of the simulation.

Figure 4 Particle model for injection molding with (a) a plate mold, (b) a mold with a corner, and (c) a mold with a branch. PP and GF denote polypropylene and glass fiber.

Figure 5 Simulated results of injection into the plate mold.

Figure 6 Fiber accumulation near the wall. Fibers #2 and #3 near the wall almost stopped during the small time increment Δt.

Figure 7 Simulated results of injection into a mold with a corner.

Figure 8 Disturbed fiber orientation near a branch. Arrows in Fig. (a) show the fibers inclined from the flow direction after passing the branches.

Figure

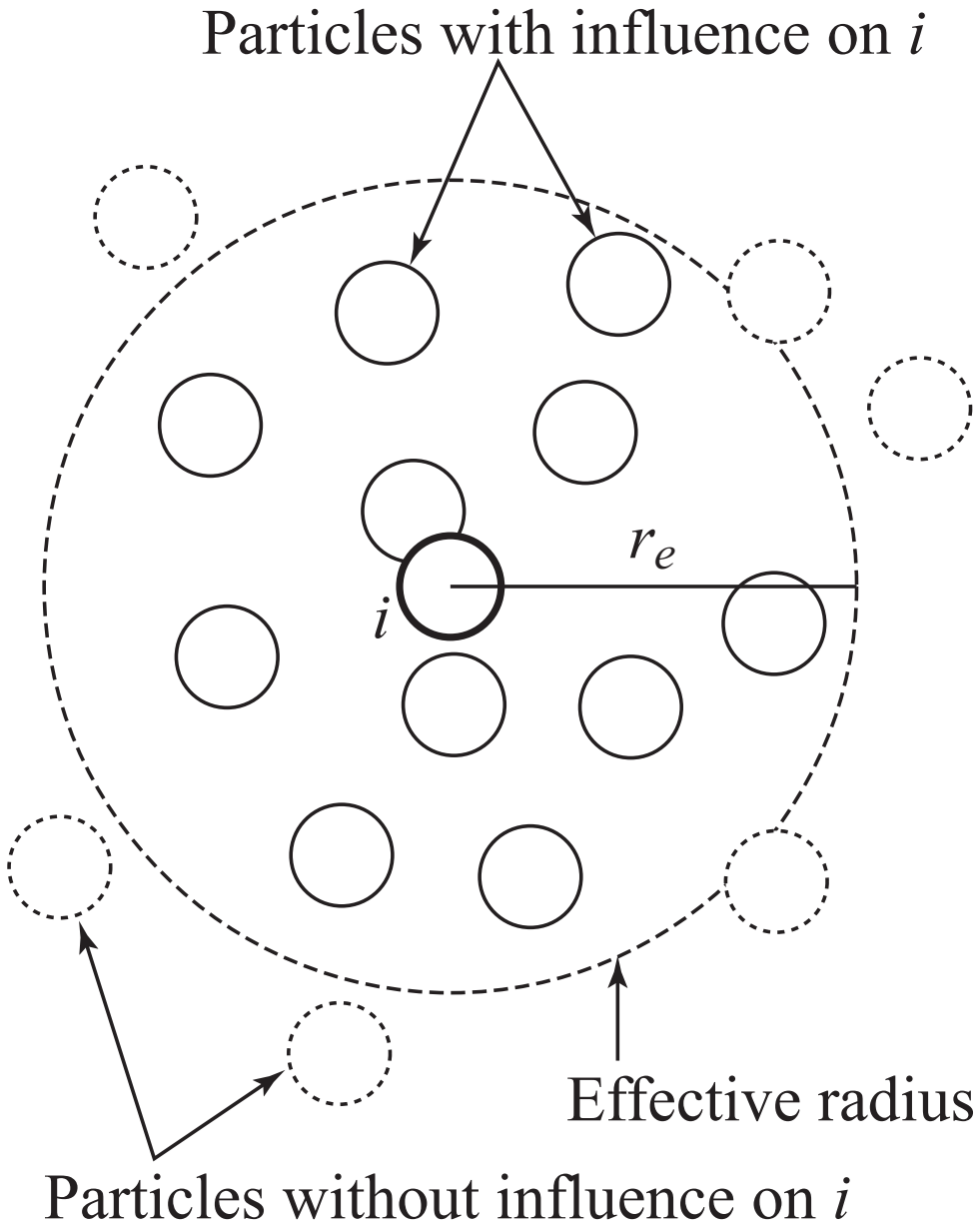

Figure 1

Figure

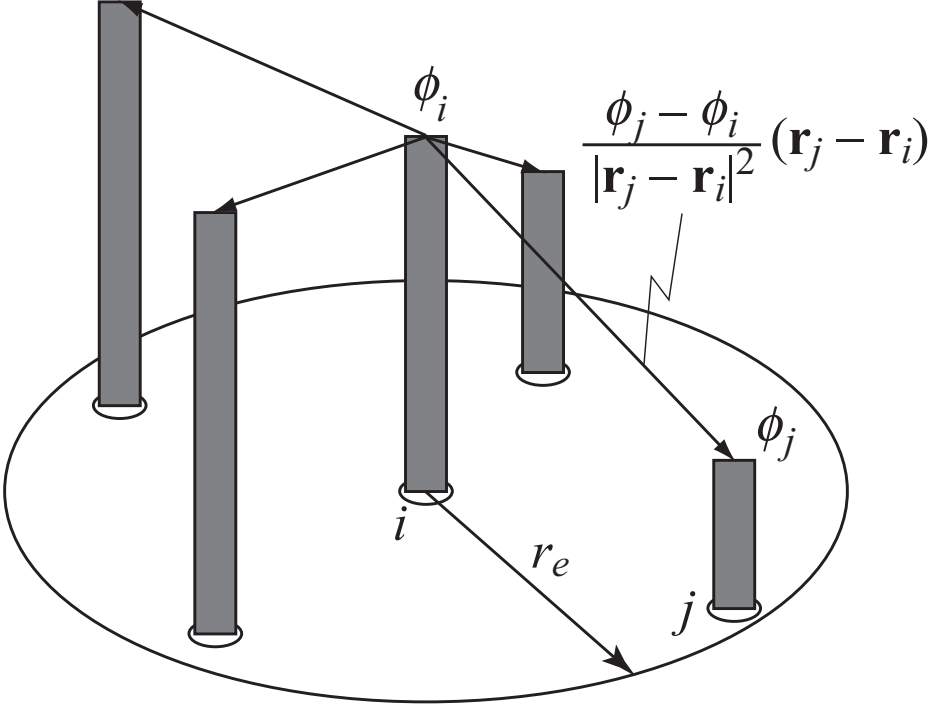

(a) Gradient model

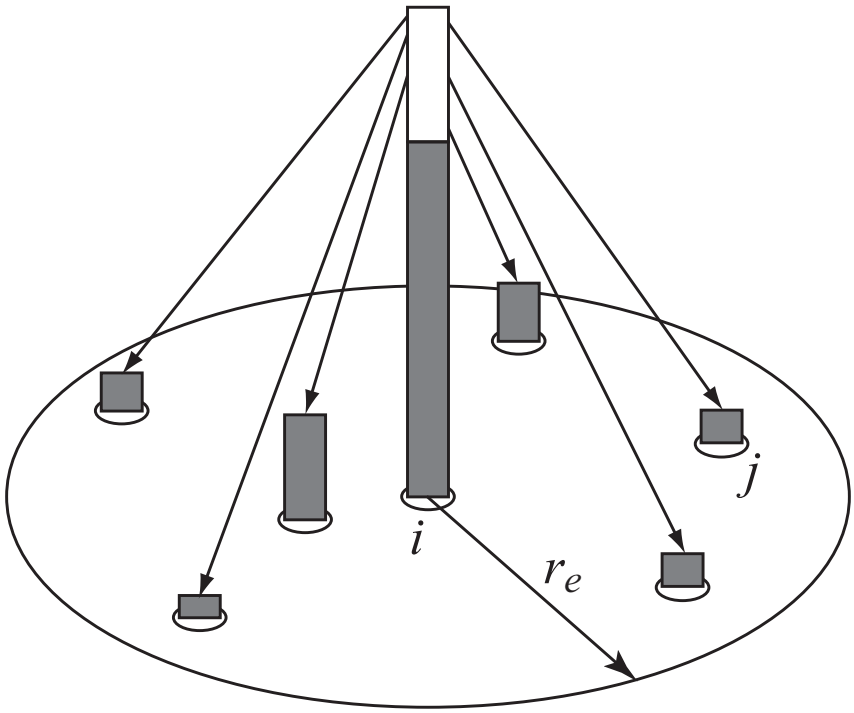

(b) Laplacian model

Figure 2

Figure

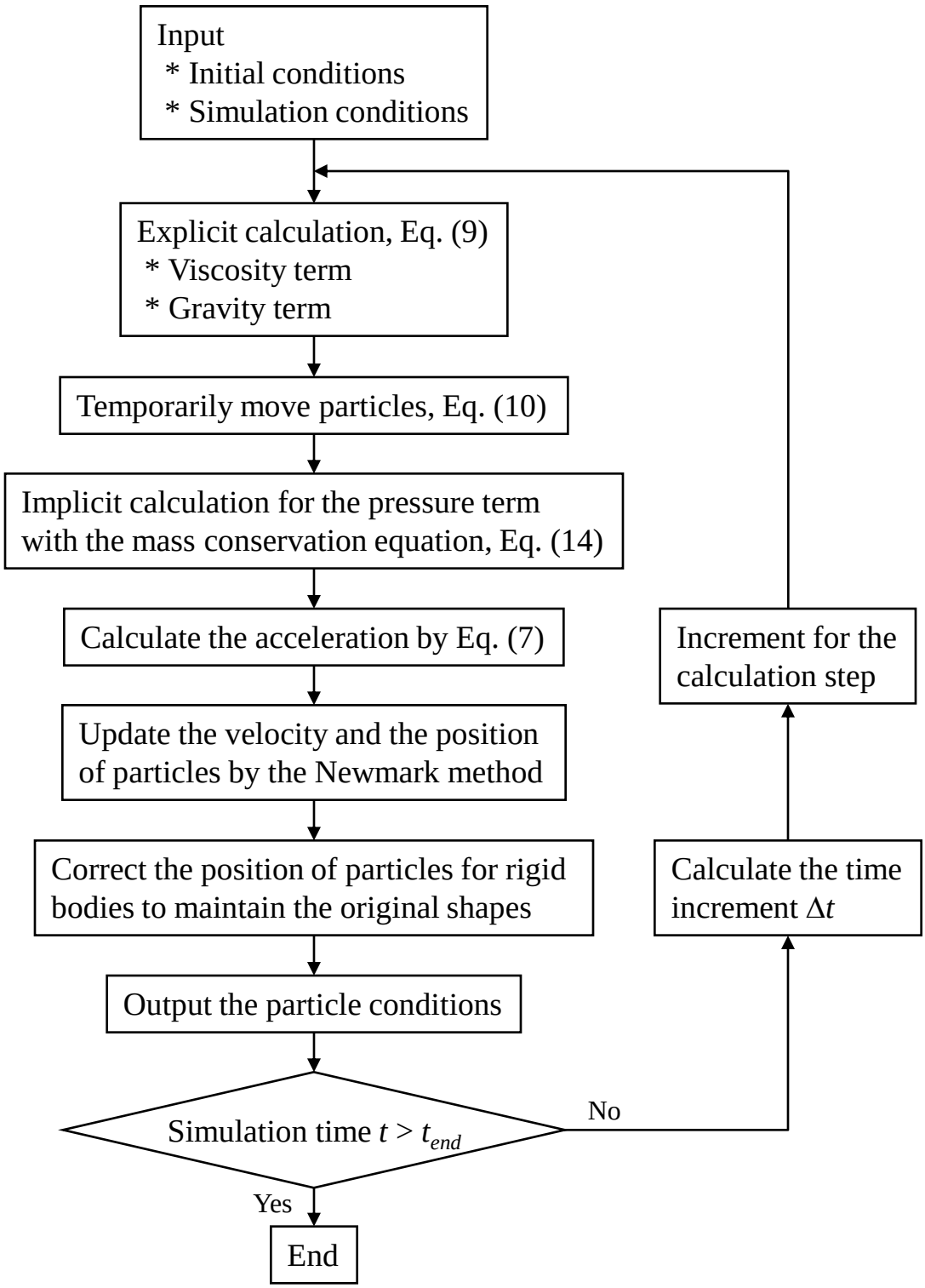

Figure 3

Figure

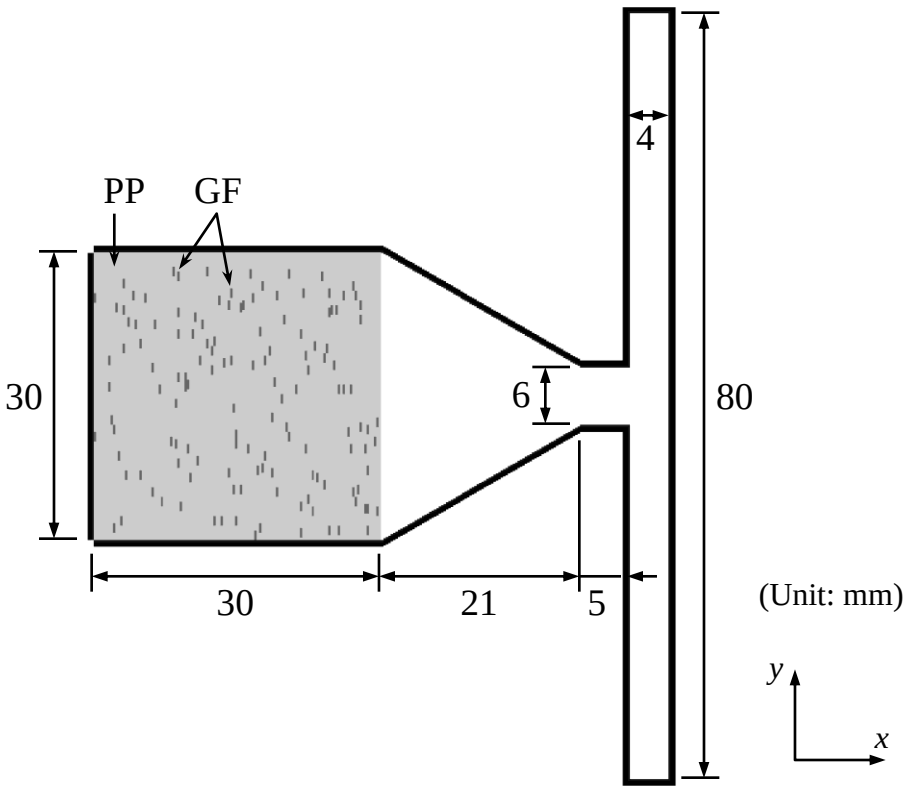

Figure 4(a)

Figure

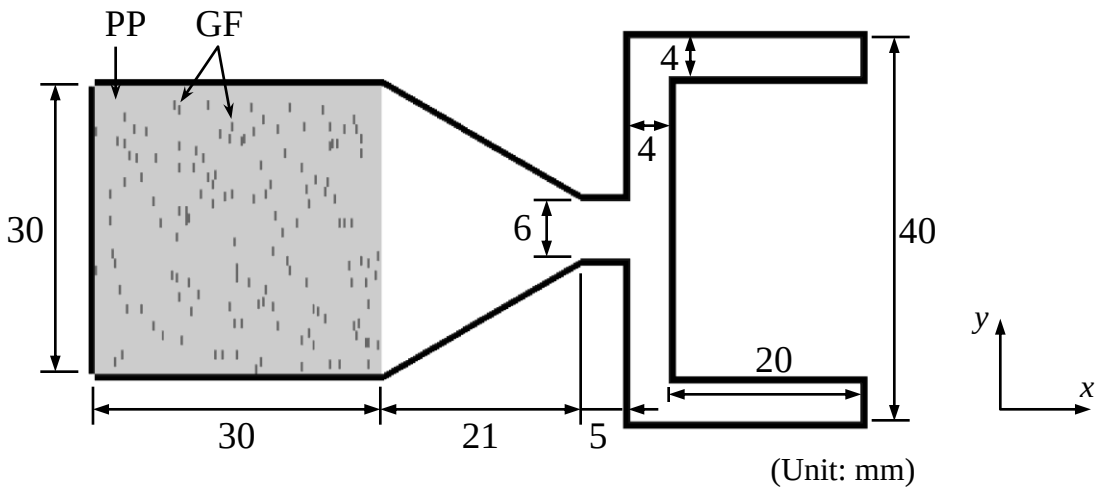

Figure 4(b)

Figure

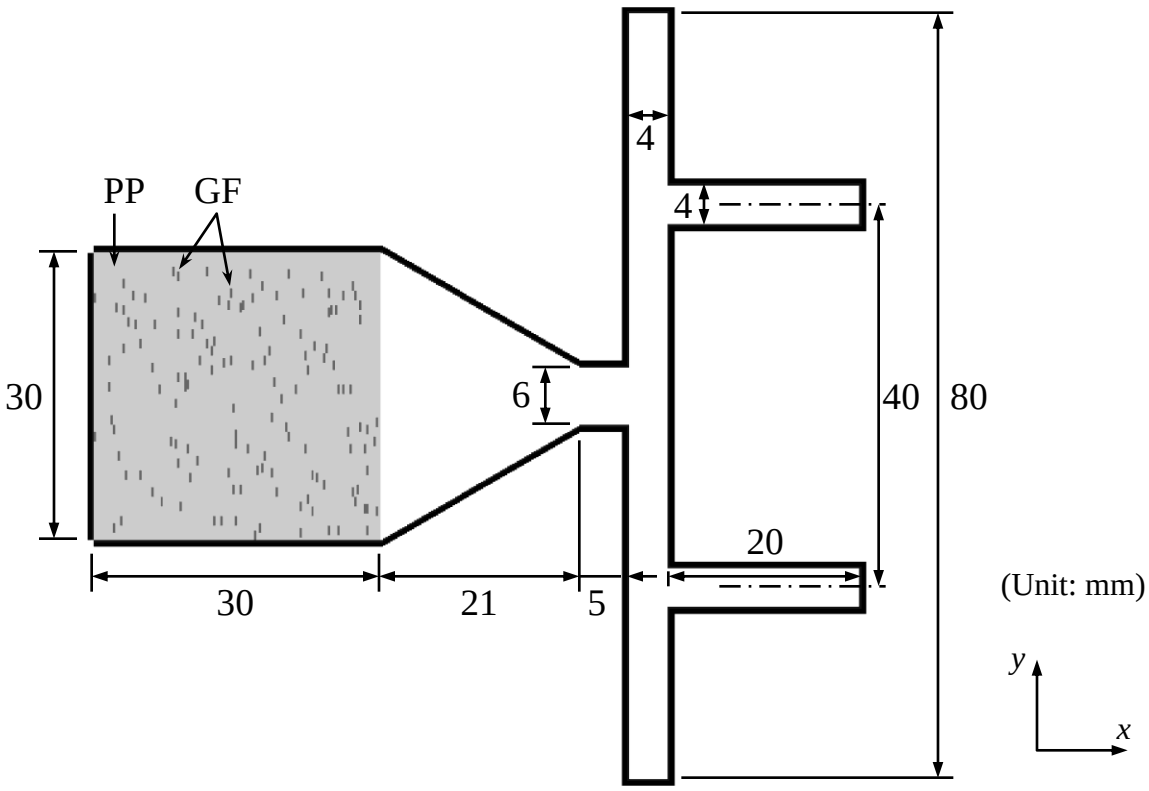

Figure 4(c)

Figure

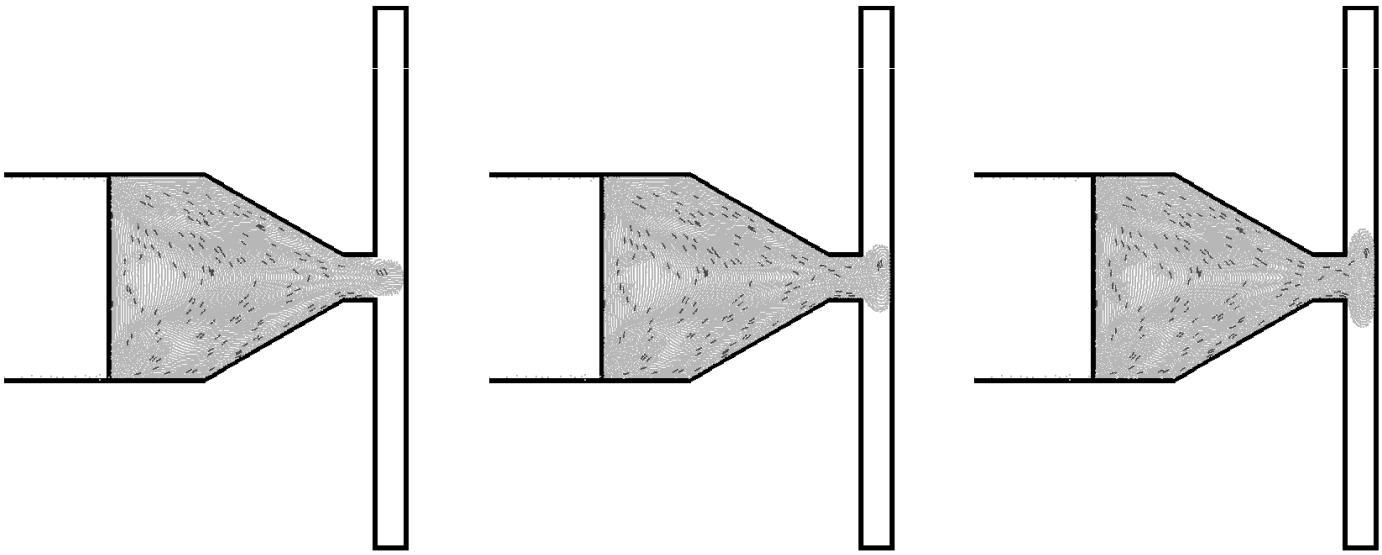

0.02 s 0.025 s 0.03 s

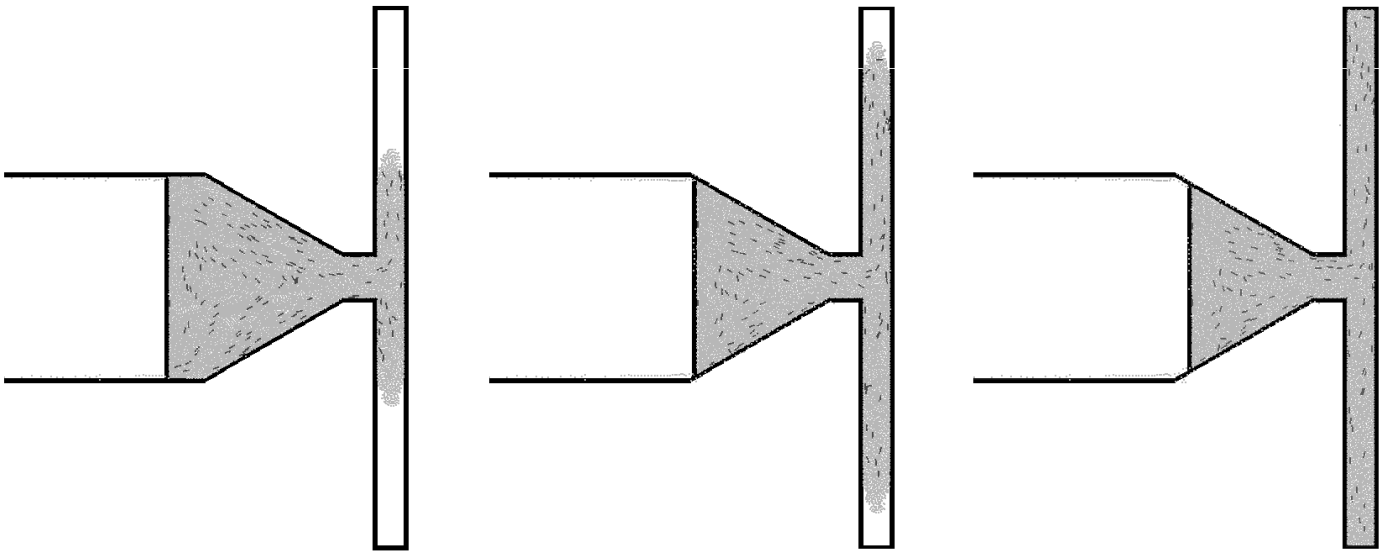

0.06 s 0.12 s 0.165 s

(a) Particle motion

Figure 5

Figure

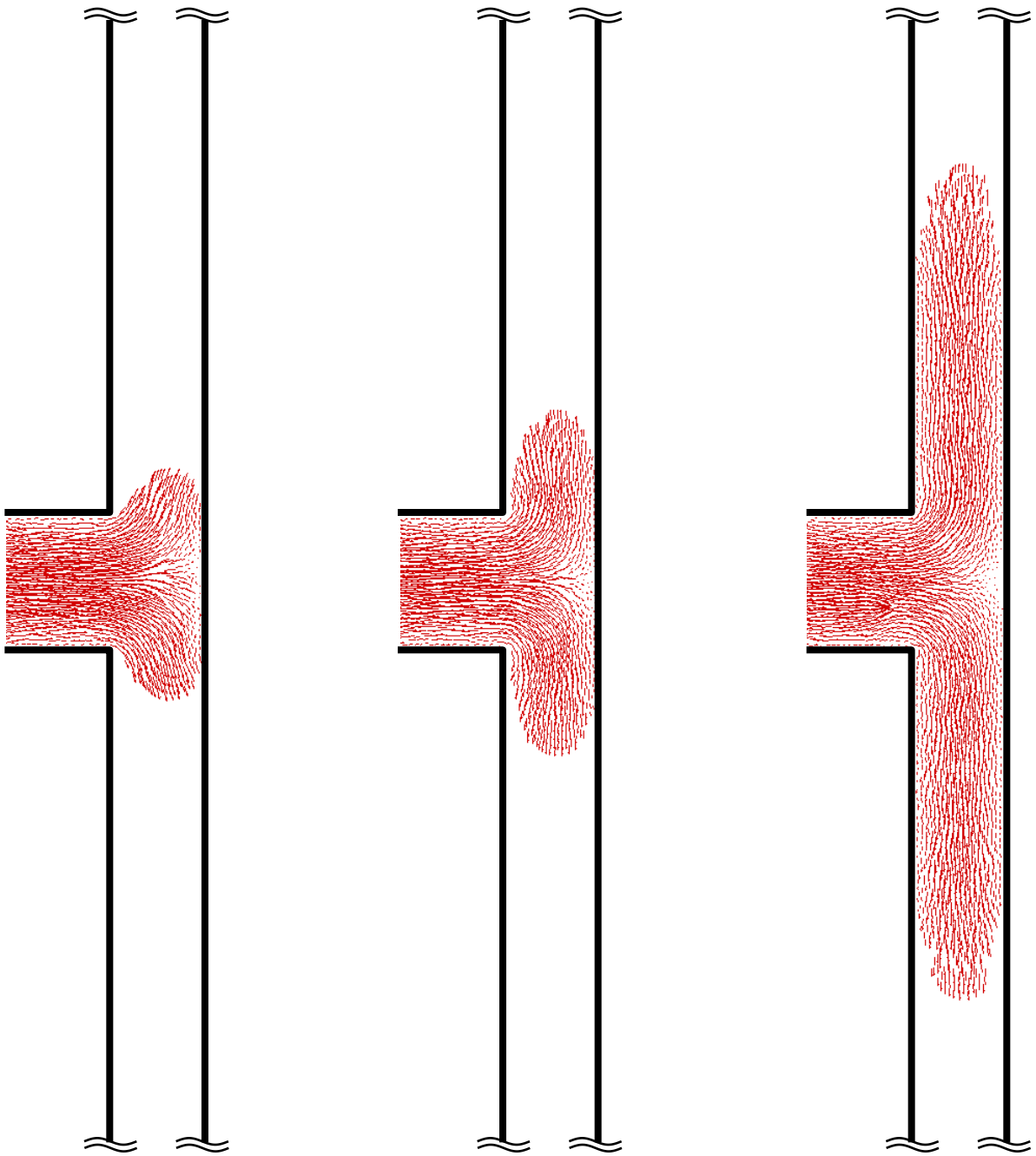

(b) Velocity distribution

Figure 5

Figure

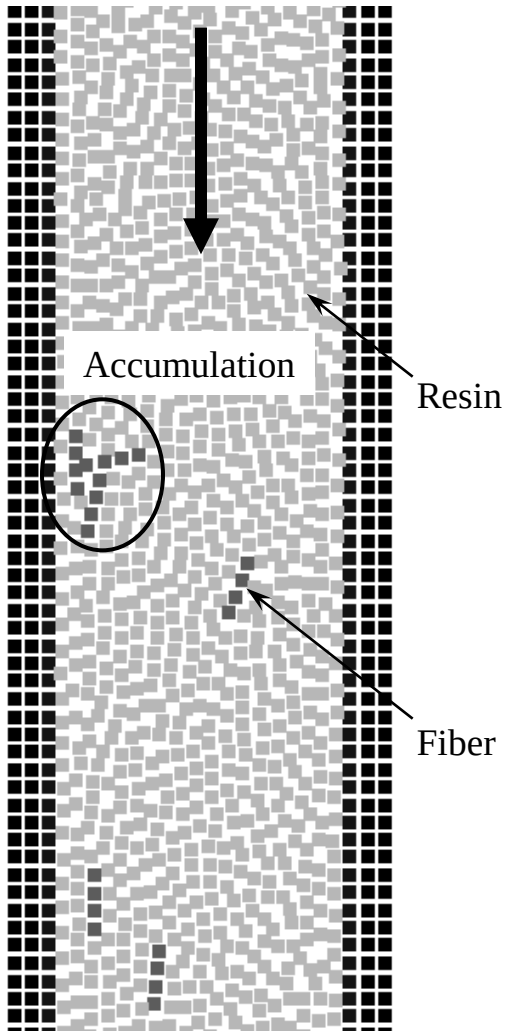

(a) Particle motion

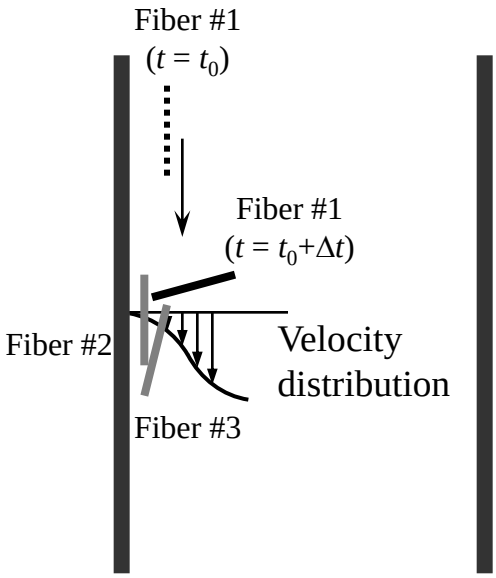

(b) Schematic

Figure 6

Figure

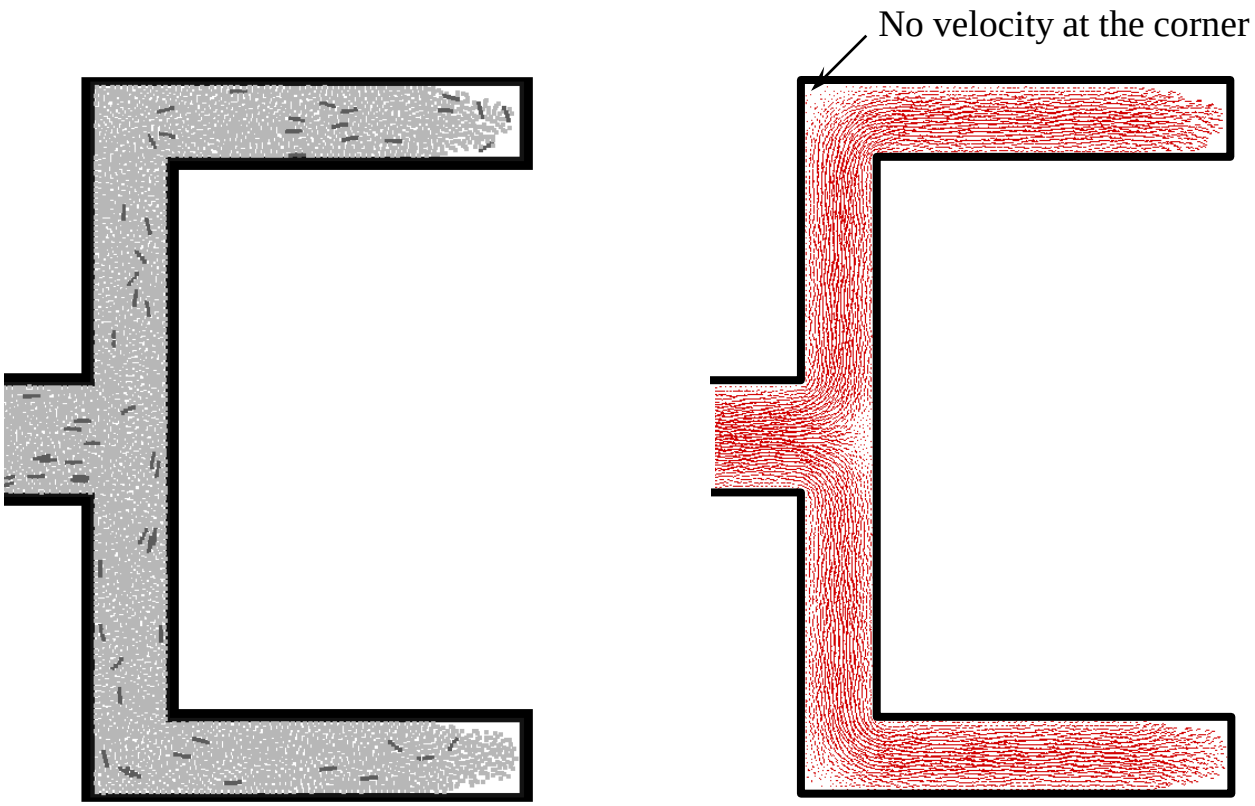

(a) Particle motion (b) Velocity distribution

Figure 7

Figure

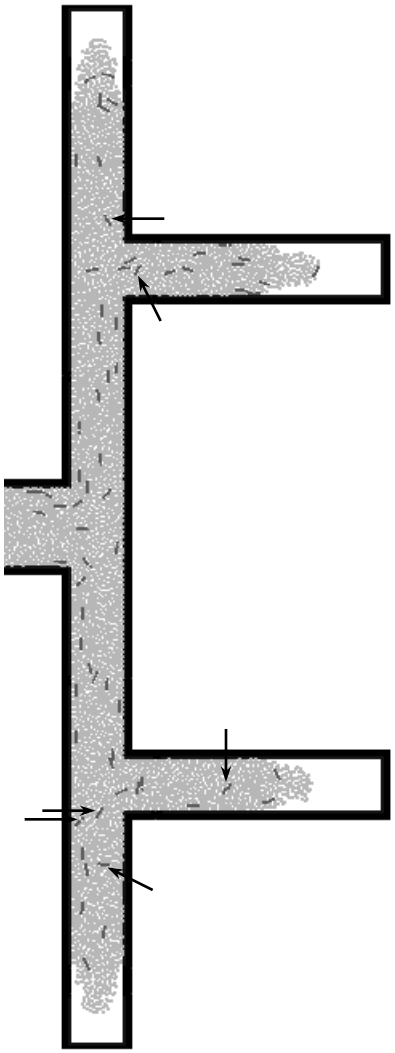

(a) Particle motion

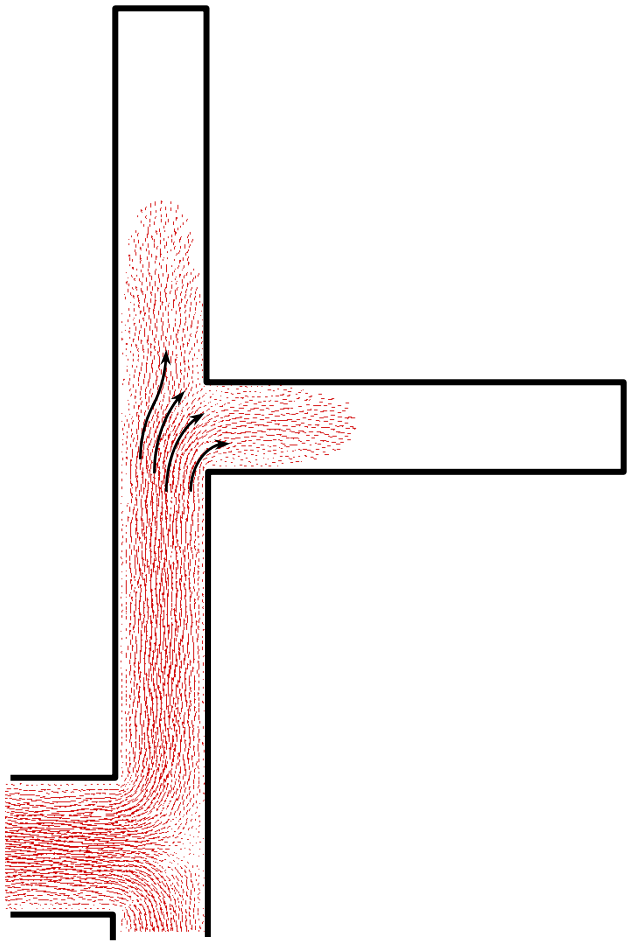

(b) Velocity distribution

Figure 8